Temperature sculpting in yoctoliter volumes

Joseph E. Reiner[1#], Joseph W.F. Robertson[2#], Daniel L. Burden[3], Lisa K. Burden[4], Arvind Balijepalli[2,5], and John J. Kasianowicz[2]

1. Department of Physics, Virginia Commonwealth University, Richmond, VA 23284.
2. Semiconductor and Dimensional Metrology Division, Physical Measurement Laboratory, National Institute of Standards and Technology, Gaithersburg, MD 20899-8120.
3. Chemistry Department, Wheaton College, Wheaton, IL 60187.
4. Biology Department, Wheaton College, Wheaton, IL 60187.
5. Laboratory of Computational Biology, National Heart Lung and Blood Institute, National Institutes of Health, Rockville, MD 20892.

[#]These two authors contributed equally.

Supporting Information

Contents **Page**

Preparation of N293C. αHL was genetically engineered to incorporate a cysteine residue on the extracellular cap of the ion channel. For this, a pair of DNA primers with a mutation site designed to replace amino acid 293 (Asn) with a cysteine were constructed and combined with a plasmid template containing wild type □HL in a polymerase chain reaction (QuikChange Site-Directed Mutagenesis Kit, Stratagene*). Genetically engineered protein αHL -N293C with an N-terminal His_6 affinity tag was expressed in *E. coli* (BL21, Novagen) and purified to homogeneity by immobilized metal affinity chromatography (IMAC) using HisTrap resin (GE Healthcare). Purified αHL -N293C was incubated with the site-specific protease AcTEV (Invitrogen) to allow removal of the N-terminal His6 affinity tag followed by further purification using IMAC. Fully processed αHL -N293C flowed through the column while contaminating His_6-tag, protease, and uncleaved αHL bound to the resin. Homogeneously purified αHL -N293C (~ 0.2 mg/ml) was stored in 20 mM Tris (pH 7.5), 100 mM KCl at 4 °C.

Temperature Calculation. The temperature of each particle was calculated from the absorbed power $P_{abs} = I_b \eta_{abs,}$ where $I_b = (P/\pi\, w_0^2)\, (1+(z\,\lambda/\pi\, w_0^2)^2)^{-1}$ is the intensity of the laser beam where P is the laser power incident on the particle, $w_0 = (3.00 \pm 0.75)$ μm is the beam waist, $\lambda = 532$ nm is the laser wavelength and z is the axial distance of the particle from the focal plane. The Rayleigh absorption cross section is given by $\eta_{abs} = (6\, n_w\, \pi\, V/\, \lambda)\, \mathrm{Im}(\varepsilon_g\text{-}\varepsilon_w/\varepsilon_g\text{+}2\varepsilon_w)$ for a sphere of volume $V = 4\pi\delta\, (a^2 - 2a\delta + 2(1- \exp(-(a/\delta))\, \delta^2)$, skin depth $\delta \approx 11$ nm at 532 nm wavelength [1] and radius $a = 20$ nm. The complex dielectric constant of the gold nanoparticles for 532 nm light is $\varepsilon_g = (-4.7 + 2.3i)$ and the water surrounding the particle is characterized by an electric permittivity $\varepsilon_w = 1.77$ and index of refraction $n_w = 1.33$ [1-4]. These parameters and equations were used to estimate the temperature of the particle.

Control Experiments. To estimate the stoichiometry of the gold nanoparticles bound to single pores, and demonstrate the selective binding of gold nanoparticles to the mutated protein nanopores, a scanning electron microscopy (SEM) experiment was performed. Because the SEM operates in a high-vacuum environment, a robust tethered bilayer membrane (tBLM) was prepared as the support for the protein-nanoparticle assembly [5-7]. The essence of the tBLM is a self-assembled monolayer of synthetic lipid with a thiolated poly(ethylene glycol) spacer HC18

(*Z* 20-(*Z*-octadec-9-enyloxy)-3,6,9,12,15,18,22-heptaoxatetracont-31-ene-1-thiol) diluted with β-mercaptoethanol, formed from a solution of 0.06 mM HC18/ 0.14 mM β-mercaptoethanol in ethanol. A bilayer was formed on this surface through the process of rapid solvent exchange. 20 μL of 10 mg/mL diphytanoylphosphocholine (DPhyPC) in ethanol was added to a dry monolayer surface and after 2 min, the solvent was exchanged with Milli-Q water (10 mL in approximately 1 min). This process results in a lipid bilayer supported on a ≈ 3 nm thick polymer cushion which is amenable for αHL pore formation [6]. 200 μL of ≈ 1 nM DNA modified N293C αHL in a pH 5.5 buffer of 0.1 M KCl; 10 mM Na(CH_3COO) and allowed to form nanopores for ≈ 24 hr. DNA modified Au nanoparticles were injected into the solution well and immediately purged from solution by washing the surface with 10 mL of Milli-Q water. The modified surfaces were then dried with compressed air and transferred into the SEM for imaging. Figure SI 1 displays a collection of images of from single particles through large aggregates suggesting that assembly of nanoparticles is not limited by electrostatic repulsion under the experimental conditions used in the paper. A total of 32, ≈ 100 μm^2 images (Figure SI 1A) were collected resulting in 419 single particles, 219 double particles, 110 triple particles (57 clustered around a central point) and 299 larger aggregates (> 3 particles). A control sample in which DNA-modified Au was exposed to a membrane with no protein nanopores and vigorously washed from the cell showed no sign of Au nanoparticles, which suggests that a large fraction of the Au in the images was bound specifically to protein that was in the tBLM (Figure SI 2B).

Several controls verified that the changes in the channel conductance resulted from the heating of gold nanoparticles attached to the ion channel. These experiments illustrate the advantage of directly attaching the heating source to the ion channel and show that in the absence of direct attachment, temperature jumps reported by the nanopore are still possible (albeit with less reproducibility). Figure SI 2A illustrates the results of a negative control in which there are no gold nanoparticles present. Specifically, the laser beam itself is not sufficient to cause the temperature increase.

Two positive controls were performed. Samples were prepared by first forming a monolayer of 20-tetra-decyloxy-3,6,9,12,15,18,22-heptaoxahexatricontane-1-thiol (WC14) [6, 8] on 40 nm Au nanoparticles. This monolayer essentially coats the nanoparticle with a lipid-monolayer which

when injected from solution in the presence of a lipid bilayer allows the Au to specifically adsorb to the membrane. Using the high temperature data reproduced from Figure 2A as a visual control in Figure SI 2B, the heating observed by illuminating a large cluster of Au is shown in Figure SI 2C (likely aggregated Au nanoparticles anchored to the membrane through WC14) rivals the temperature changes reported in the paper, but with less stability in the in the high-temperature state. It is likely that the αHL occasionally diffused near Au clusters in the membrane, and the distance between the heat source and the ion channel varied over the course of the experiment. When a lower density of Au is added to the membrane (Figure SI 2D), there is little to no observable heating from isolated nanoparticles. This suggests that in the absence of any aggregation of Au nanoparticles, there is essentially no added heating due to Au that is not directly attached to the protein.

Fitting time constants. The observed time constants for these experiments were estimated as a series of 2 time constants for the low frequency data and 3 time constants for the high frequency data. In each case, the fastest time constant was considered a sigmoidal function with τ equal to the bandwidth of the Bessel filter. The equation used was

$$\Delta I_{f(T)} = a\left(\frac{1}{1+\exp\left(-\frac{t-d}{t_1}\right)}+\left(1-\exp\left(-\frac{t}{t_2}\right)\right)+\left(1-\exp\left(-\frac{t}{t_3}\right)\right)\right)+b$$

where $\Delta I_{f(T)}$ is the temperature dependent current, α is a scaling constant, t is the time from the temperature step, δ is a bandwidth-limited delay, τ_1, τ_2 and τ_3 are time constants and b is a linear offset. To reduce the uncertainty and provide an estimate of the error temperature steps were averaged prior to fitting to the equation. For the low frequency data 3 sets of 130 steps were fit and for the high frequency data 6 sets of 500 steps were fit. Error bars are the standard deviation of the estimated fit parameters.

Table 1: estimated time constant from a single channel with low frequency sampling: 50 kHz sampled data/ 10 kHz filtered

	α μ±1σ (pA)	δ μ±1σ (ms)	τ_1 μ±1σ (ms)	τ_2 μ±1σ (ms)
Up	48.3 ± 0.3	0.51 ± 0.02	0.1+/-0.0	1.16 ± 0.05
Down	-48.0 ± 0.1	0.41 ± 0.07	0.1+/-0.0	1.10 ± 0.02

Table 2: estimated time constant from a single channel with high frequency sampling 250 kHz sampled data/ 100 kHz filtered.

	α μ±1σ (pA)	δ μ±1σ (ms)	τ_1 μ±1σ (ms)	τ_2 μ±1σ (ms)	τ_3 μ±1σ (ms)
Up	45 ± 1	0.055 ± 0.001	0.01+/-0.0	0.046 ± 0.001	0.348 ± 0.008
Down	-44 ± 1	0.025 ± 0.001	0.01+/-0.0	0.016 ± 0.001	0.307 ± 0.005

Residence time estimation. To calculate the expected residence time of the PEG29 molecules in the nanopore, we used a model for PEG interactions with both the pore and cations [9]. We used the following values for the parameters in the model: k_BT_{room} = 25.4 meV, a^* = 1.23, b^* = 1.15, s^+ = 0.229, s^{PEG} = 0.129, ΔG_o = -52.0 meV, ξ = 7.07 Vs/m, x = 4.81 and ΔG_c = 1.03 meV modified from the original fit in 4M KCl in [9]. Where k_BT_{room} is the thermal energy at room temperature, a^* and b^* are effective diffusion coefficients given by $a^* = \left(D_+^{eff} + D_-^{eff}\right) / D_0$ and $b^* = D_+^{eff} / D_0$ where $D_\pm^{eff}$ is the effective diffusion parameter in the PEG occupied region of the pore for cations (+) and anions (-) and D_0 is the diffusion coefficient for all ions in the unoccupied pore, s^+ is a correction factor for the electroosmotic force to the electrical force on a single cation, s^{PEG} is a correction factor for the electroosmotic force to the electrical force on the entire PEG molecule, ΔG_o is the free energy of PEG-cation binding inside the pore, ξ is the hydrodynamic drag term, x is the mean number of monomers bound to a single cation and ΔG_c is the free energy of confinement of polymer in the pore. While the fit parameters to the model might depend on the cation concentration, we ignore that possibility here and set the KCl concentration to 3M and adjust the temperature (k_BT) accordingly. Nevertheless, our model reasonably explains the qualitative trend in the observed residence time as a function of solution temperature.

* Certain commercial equipment, instruments, or materials are identified in this paper in order to specify the experimental procedure adequately. Such identification is not intended to imply recommendation or endorsement by the National Institute of Standards and Technology, nor is it intended to imply that the materials or equipment identified are necessarily the best available for the purpose.

References

1. Seol, Y., Carpenter, A. E., Perkins, T. T. *Opt. Lett.* **1996**, *31*,2429–2431.

2. Svoboda, K., Block, S. M. *Opt. Lett.* **1994**, *19*,930–932.

3. Johnson, P., Christy, R. *Phys Rev B* **1972**,*6*,4370–4379.

4. Coronado, E. A., Encina, E. R., Stefani, F. D. *Nanoscale* **2011**, *3*, 4042.

5. He, L.; Robertson, J. W. F.; Li, J.; Karcher, I.; Schiller, S.; Knoll, W.; Naumann, R. L. C. Langmuir 2005, 21, 11666–11672.

6. McGillivray, D. J.; Valincius, G.; Heinrich, F.; Robertson, J. W. F.; Vanderah, D. J.; Febo-Ayala, W.; Ignatjev, I.; Lösche, M.; Kasianowicz, J. J. *Biophys. J.* **2009**, *96*, 1547–1553.

7. Vockenroth I.K., Ohm, C., Robertson, J. W. F., McGillivray, D. J., Lösche, M., Köper, I. *Biointerphases* **2008**, *3*,FA68.

8. McGillivray, D. J., Valincius, G., Vanderah, D. J., Febo-Ayala, W., Woodward, J. T., Heinrich, F., Kasianowicz, J. J., Lösche, M. *Biointerphases* **2007**, *2*,21–33.

9. Reiner, J. E.; Kasianowicz, J. J.; Nablo, B. J.; Robertson, J. W. F. *Proc. Natl. Acad. Sci. U.S.A.* **2010**, *107*, 12080–12085.

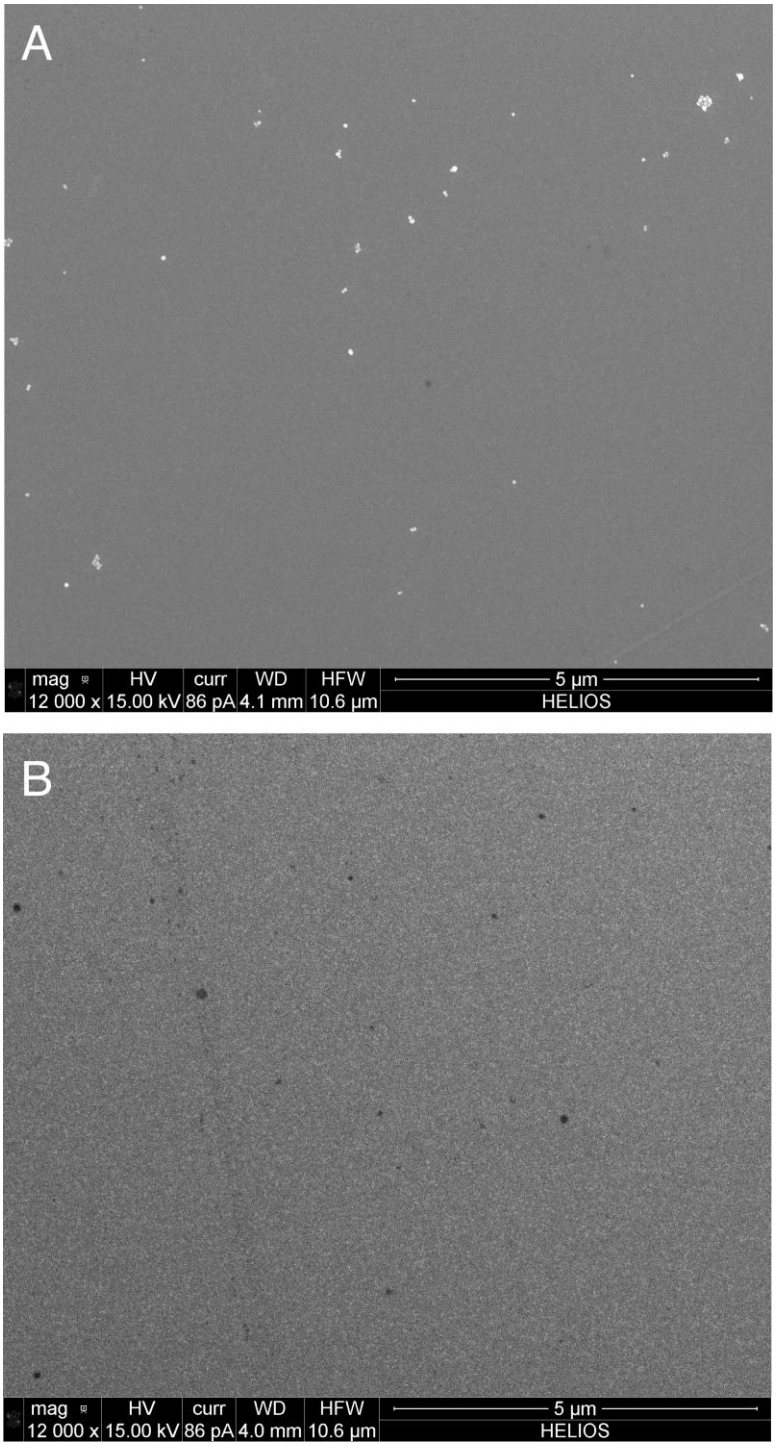

Figure SI 1. Examples of Au nanoparticle aggregates observed after attachment of complementary DNA-modified Au and N293C protein. (A) Representative image when both DNA-modified protein and DNA-modified Au are present. (B) Identical preparation as in (A), with no protein immobilized in the membrane.

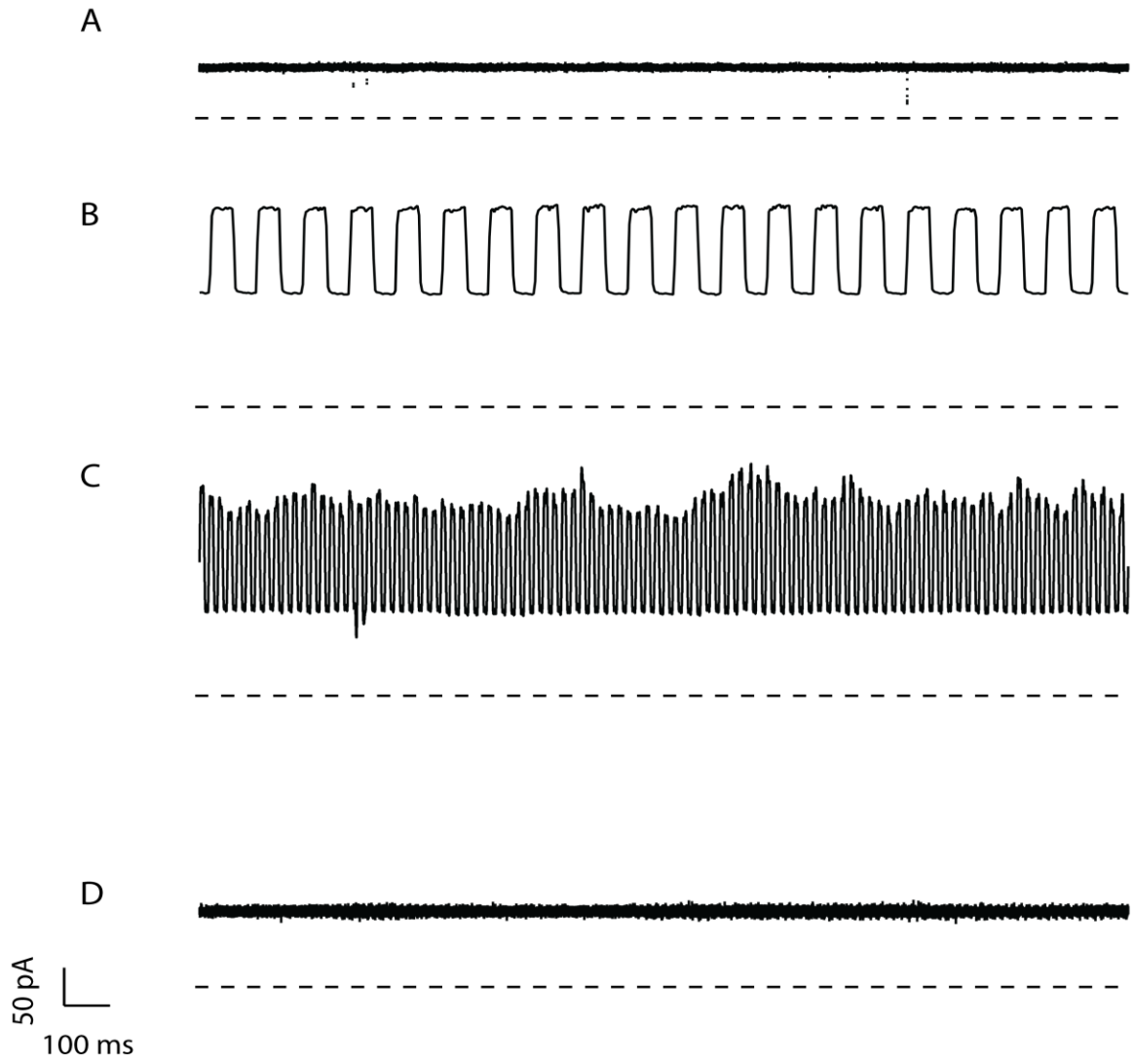

Figure SI 2. Control experiments for gold nanoparticle attachment to single nanopores. (A) A single N293C αHL ion channel without gold nanoparticles is not heated by the laser (ca. 205 mW, 40x objective). (B) Two ion channels with 40 nm gold attached through a 10 nm DNA linker (data reproduced from Figure 2a) at 197.4 mW, 40x objective, 10 Hz. (C) A single ion channel adjacent to a large gold aggregate anchored to the membrane with a thio-lipid (1, 2) at 14 mW, 10x objective, 50 Hz. (D) A single wild type-αHL nanopore in a membrane with 40 nm Au nanoparticles specifically adsorbed to the membrane through a thio-lipid illuminated with 180 mW; 40x objective, 20 Hz.

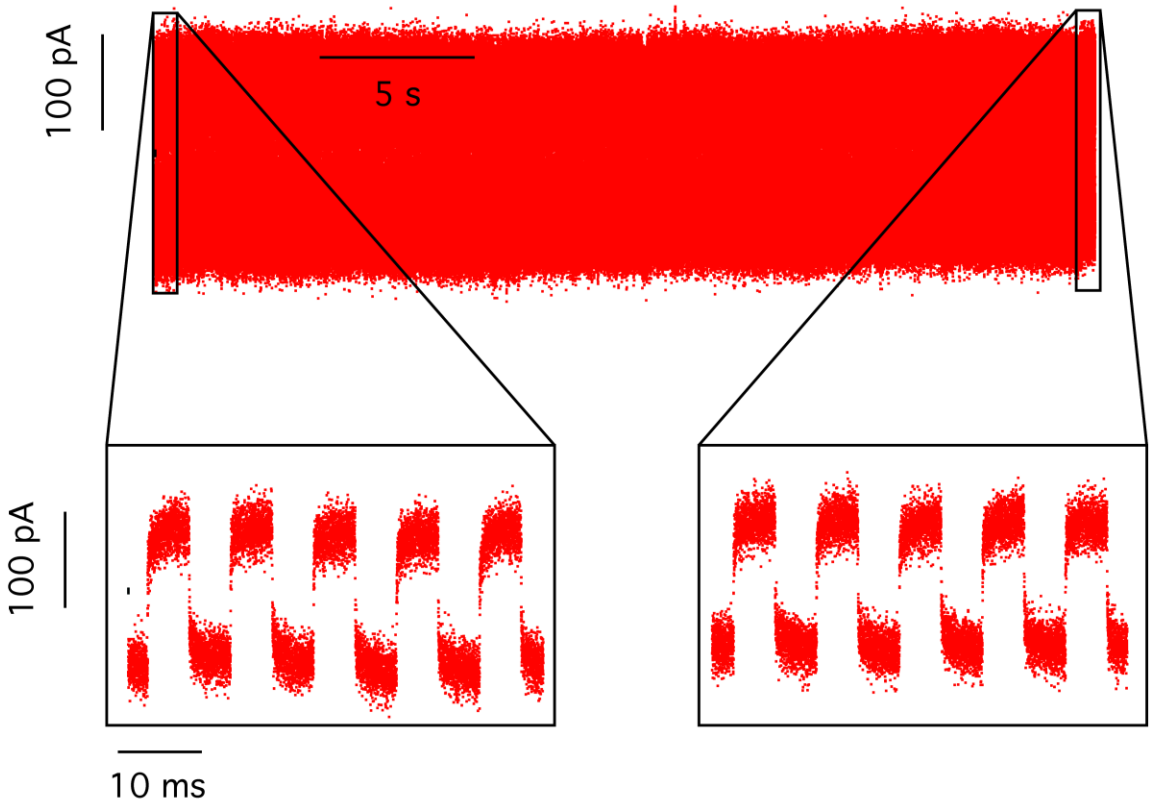

Figure SI 3. The nanopore ionic current was stable over many repeated temperature cycles. The applied potential was 40 mV and the laser illumination was cycled on and off at 100 Hz.